

Structure-Based Virtual Screening, Insilico Docking, ADME Prediction, and Molecular Dynamics Studies for Identification of Potential NMT Inhibitors Against Malaria

Mohan Anbuselvam (✉ mohanbio33@gmail.com)

Selvamm Arts and Science College

Katherine, C Ji

Drexel University

Anbuselvam Jeeva

Bharathidasan University

Hai-Feng Ji

Drexel University

Research Article

Keywords: Malaria, Plasmodium vivax, NMT, Virtual screening, Molecular Dynamics Simulation.

Posted Date: December 29th, 2021

DOI: <https://doi.org/10.21203/rs.3.rs-1199949/v1>

License: © ⓘ This work is licensed under a Creative Commons Attribution 4.0 International License.

[Read Full License](#)

Structure-based virtual screening, insilico docking, ADME prediction, and molecular dynamics studies for identification of potential NMT inhibitors against malaria

Anbuselvam Mohan^{1*}, Katherine, C. Ji^{2**}, Anbuselvam Jeeva³, Hai-Feng Ji²

¹Department of Biotechnology, Selvamm College of Arts and Science, Namakkal-637 003, Tamil Nadu, India.

²Department of Chemistry, Drexel University, Philadelphia, PA 19104, USA.

³Department of Animal Science, Bharathidasan University, Tiruchirappalli, Tamil Nadu, India.

Corresponding Author* - E-mail: mohanbio33@gmail.com

** : Equal to first author

A. Mohan

Assistant Professor

Department of Biotechnology

Selvamm Arts and Science College

Namakkal-637 003

Tamil Nadu, India.

Abstract

One of the major public health problems globally, malaria, is mainly caused protozoan parasites from the genus *Plasmodium*, and commonly spreads to people through the bites of infected female mosquitoes of the genus Anopheles. Strategies for treatment, prevention, and control are available for malaria but the eradication of malaria still poses great challenge due to plasmodium's drug resistance over the past decades. Development of novel antimalarial drugs remains a significant task to protect people from malaria. N-Myristoyl transferase is responsible for the N-Myristoylation catalysis process and the survival of Plasmodium species. Thus, it is considered a therapeutic drug target in protozoans and was recently validated as a significant target for *Plasmodium vivax*. In this present scenario, we endeavour to identify effective NMT inhibitors to prevent the onset of malaria in the human species. Initially, the structure-based virtual screening was executed against ZINC database and four potential candidates for NMT were identified. Furthermore, the four identified compounds were subjected to ADME prediction and all the four compounds found within adequate range with predicted ADME properties. Eventually, we conducted the molecular dynamics simulation to investigate the binding stability of top three protein-ligand complexes at different time scale by employing the tool Desmond. The molecular dynamics simulation studies revealed the protein-ligand complexes were stable throughout the entire simulation. Besides, we noticed that the residues ASN 365, PHE 103 and HIS 213 of NMT were crucially involved in the formation of various intermolecular interactions, significantly contributing to the stability of protein-ligand complexes. From this computational investigation, we suggest that the three identified potential compounds are extremely useful for further lead optimization and drug development.

Key Words: Malaria, *Plasmodium vivax*, NMT, Virtual screening, Molecular Dynamics Simulation.

Introduction

Protozoan parasites are one of the key causative agents of global transmittable diseases. Annually, millions of people are affected by infectious diseases such as malaria, predominantly in tropical and sub-tropical regions of the world, as well as a major life-threatening disease in developing countries. Malaria is one of the most prevalent and deadliest vector-borne diseases across human history and it mainly caused by single-celled eukaryotic protozoan parasites belonging to the genus *Plasmodium*. According to WHO, it is estimated 229 million cases of malaria and 409,000 malaria-related deaths were reported in 2020 [1]. Children aged below 5 years old and pregnant women are mainly affected by malaria due to weakened immunity. Worldwide, 67% of all malaria-related deaths occurred below age group five, also a leading cause in child mortality. It is estimated that every 45 seconds a child deceases of malaria. Malaria is mainly spread to people through the bites of infected female *Anopheles* mosquitoes.

So far, there are five identified parasite species that play a major role in malaria spread through humans, known as *Plasmodium falciparum*, *Plasmodium vivax*, *Plasmodium ovale*, *Plasmodium malariae*, and *Plasmodium knowlesi*. Various strategies for controlling and protecting against malaria have reduced the number of yearly global malaria infections by 37%, and mortality rates have decreased by 60%. However, malaria cases have steadily risen in Africa since 2014 due to drug resistance in parasitic strains [2]. Among the five species, *P. falciparum* and *P. vivax* are the two greatest contributors for malaria and highest mortality rate to human, two species that have been confirmed to have developed a resistance to current antimalarial drugs [3]. Currently, *Plasmodium vivax* is the most prevalent and the cause of most malaria-related deaths across Sub-Saharan Africa.

Plasmodium parasites are transmitted to humans through the bite of female *Anopheles* mosquitoes. Soon after transmission, malaria parasites travel through the blood stream to the

liver where they may infect a single hepatocyte. During the intracellular plasmodium infection life cycle, the malarial parasite replicates its genome over 2-10 days, and produces tens of thousands of replicated daughter parasites named merozoites. Once mature, sexual forms return to the circulation and are transmitted and expose malarial symptoms, including fever, cold, rigor, fatigue, headache, bitter tongue, vomiting, diarrhoea, convulsion, anemia, cocacola urine, hypoglycemia, prostration, and hyperpyrexia [4, 5].

Researchers have long studied malaria at multiple stages of the life cycle since addressing regulatory proteins involved in parasite transmission might provide the most robust approach to eradicate malaria transmission, infection, disease. *N*-Myristoyltransferase, or, NMT, is present in eukaryotes and was first discovered in *Saccharomyces cerevisiae*. *N*-Myristoyltransferase is a monomeric enzyme responsible for *N*-Myristoylation i.e. the co- and post-translational attachment of the C₁₄ fatty acid myristic acid to the *N*-terminal glycine of substrate protein by an amide bond, playing a critical role in assembling the inner membrane complex essential to the parasite's life cycle. There are several proteins involved in the *N*-Myristoylation process. In malaria, calcium-dependent protein kinase 14 and glideosome-associated protein 455 are essential for myristoylation to perform their biological activities. Inhibiting the catalysis of NMT can prevent *N*-Myristoylation through multiple pleiotropic downstream pathways, resulting in rapid and irreversible cell death in *Plasmodium* species. NMT is one of the well-validated drug targets for the development of anti-malarial drugs. Several research groups also attempted to explore potential inhibitors against NMT through computational approaches [6, 7, 8]. Some of the previously described inhibitors are active against blood stage of the *Plasmodium vivax*.

Plasmodium vivax has become resistant to previously successful identified drugs, including chloroquine, primaquine and sulphadoxine-pyrimethamine, and many calls have been made for new anti-malarial drug targets [9, 10]. There is an urgent need to introduce anti-

malarial drugs in hopes to overcome the drug resistance and eradicate malaria both effectively and efficiently.

In this present study, we employed structure-based virtual screening of molecules in the Zinc database, which allowed us to study the best interactions and affinity between known ligands that may be used as drugs with their molecular target, NMT. The most successful retrieved hit compounds were consequently subjected to molecular docking, ADME properties, and molecular dynamic simulation studies.

Materials and Methods

Virtual screening

Structure-based virtual screening has been widely employed in early stages of the drug discovery for the identification of new effective ligands with high affinity for therapeutic targets. The X-ray crystal structure of NMT was retrieved from the Protein Data Bank under code: 4A95 with high resolution 1.55Å [11]. Target structures were then prepared and refined using the Protein Preparation Wizard implemented in the Schrödinger suite. In this pre-processing step, we employed some certain criteria, including (i) addition of a hydrogen atom, (ii) missing atoms and side chain residues were added and proper partial charges were assigned (iii) disulphide bonds were created, and iv) unwanted water molecules were removed from the target structure. Next, the pre-processed target protein structure was optimized with PROPKA and the energy was minimization was done by employing force field OPAL3 until the convergence of heavy atoms of RMSD reached 0.3 Å. Then, the refined target structure was taken into Glide receptor grid generation panel for the generation of the three-dimensional (3D) grid box with a size of 20 × 20 × 20 Å with van der Waals scaling factor set at 1.0 and partial charge cut-off at 0.25. A total of 300,000 compounds were downloaded from Zinc database in the form of SDF and the compounds structure were imported into ligprep panel and preparation was performed [12, 13]. Here we applied some crucial criteria for ligand

preparation including i) Ligands ionization points at $\text{pH } 7.0 \pm 2.0$ and the stereoisomers were generated for each ligand structure, ii) compounds structural energy minimization using the OPLS3 force field, (iii) the *desalt*-option were generated, (iv) tautomer were generated for all conformers, (v) one lowest energy conformer was generated per ligand. Then the prepared target protein and drug compounds structures are input file for structure based virtual screening. In this study, we employed the most efficient computational tool glide for virtual screening; the glide offers three significant filtering steps: HTVS, SP and XP. The high-throughput virtual screening mode was used for efficiently enriching millions of compound libraries, the standard precision mode was used for reliably docking tens to hundreds of thousands of ligands with high accuracy, and finally we applied the extra precision mode for further elimination of the unwanted compounds [14].

Drug Likeness Properties Prediction

Nowadays, many drug discovery research groups invest a large amount of money and time to invent more effective drug candidate for therapeutic targets with desired pharmacology activities. However, many chemical agents do not come to market as commercial product and produce their anticipated pharmacology efficiency against validated therapeutic targets following clinical trials. Nearly 60% of the drugs fail to attain proper potency in clinical trials due to poor solubility, permeability, and toxicity rates. Generally, molecules with inadequate ADME properties extend the experimental process. An ideal drug possesses not only effective pharmacological action but it having some additional quality like bioavailability and safe toxicological profile [15]. Experimental ADME determination is not suitable for all newly invented chemical entities due to expensive, lengthy process, and animal wastage. Due to this reason pharmaceutical researchers commonly depend on *in silico* ADME tools to evaluate the ADME profile. The ADME filtration approach is widely applied in early stages of drug discovery and development process to predict whether the chemical compounds are probable

effective drug candidates and will be able to effectively reach the target site and produce their pharmacological action, elicit from accumulation and toxic effects [16]. Here we employed Qikprop for ADME properties estimation. Qikprop is mostly recommended familiar insilico tool by drug discovery group because of its ease of use as well as its efficient predictions with credible properties. We appraised the following partition coefficient (QPlogP octanol/water): the water solubility (QP log S), gut-blood brain barrier (QPPCaco2), LogIC50 value for blockage of K⁺ channels (QPlogHERG), percentage of human oral absorption, molecular weight, hydrogen bond donor, hydrogen bond acceptor, number of rotatable bonds, and Madin-Darby Canine Kidney cells (MDCK) [17].

Molecular dynamics simulation

Biological macromolecules undergo significant conformational changes before initiating their crucial biological activity. The conformational changes occur inside the organism due to enzymatic activation via mutation, phosphorylation, protonation, or the addition or removal of a ligand. Understanding the behaviour of the macromolecule-ligand interaction at an atomic level is crucial for understanding the nature of molecular biology for various molecules [18]. Here, MD simulations were performed by the computational tool Desmond to determine the conformational change, ligand binding, binding stability, and variability of top-ranking docked complexes [19]. The system builder panel was employed to generate orthorhombic simulation box with SPC model. The surface of the protein and simulation box distance was maintained at 10Å. Further, the systems were neutralized by adding adequate number of Na⁺ and Cl⁻ ions. The energy minimized system subsequently took into 100ns molecular dynamics simulation execution with NPT ensemble at constant temperature of 300 K and 1.01325 bar pressure over 100 ns with recording intervals of 1.2 ps for energy and 100 ps for trajectory. The simulation was run with the help of OPLS-3e force field [20]. Eventually, the RMSD, RMSF and various intermolecular contacts of the top

ranked docked complexes were observed with the help of simulation interaction diagram panel.

Results and Discussion

Selection of NMT inhibitors

In order to find potential inhibitors against NMT in efforts to eradicate malaria; we performed a virtual screening computational approach against the ZINC database. We employed Glide to execute virtual screening for rapid ligand filtration, efficacy, and accuracy of binding affinity. The Glide tool possesses multi-step ligands filtration which included high throughput virtual screening (HTVS), standard precision (SP) and extra precision (XP). In order to evaluate the potency of the Glide docking tool, initially, we downloaded crystal structure of NMT (PDB: 4A95) from PDB, extract the co-crystal inhibitor quinoline from the active site of the target structure of NMT and re-docked into same position of NMT by using three different glide docking modes; the binding free energy observed for each mode of docking were -5.21kcal/mol, -7.32kcal/mol, and -8.43kcal/mol and further utilized for database screening. Then, we superimposed the native crystal structure with re-docked structure. The RMSD of the superimposed structure was found to be 0.213Å. Residues GLY 386, GLY 199, and ASN 365 were involved in the formation of various interactions with the molecules. The results clearly indicate Glide docking protocol is more dynamic for further screening processes.

In the first step of the database screening, the prepared compounds were docked into active site region of the NMT. We filtered out 50,000 in the first step of the database filtering on HTVS, then sorted out 16,450 compounds from SP mode of the Glide and 1003 compounds from the Glide XP mode. The compounds were further considered ADME drug-like predictions for further filtration. In this drug-like filtering phase we screened four potential compounds for NMT based on the predicted ADME properties, comprised of

Compound 1: ZINC37555319: N-{4-[(benzylcarbamoyl)methyl]phenyl}-N-[(4-methylphenyl)methyl]furan-2-carboxamide, Compound 2: ZINC41016284: 2-(1,3-Dioxo-1,3-dihydro-isoindol-2-yl)-4-methyl-pentanoic acid [4-(4-fluoro-phenyl)-5-methyl-thiazol-2-yl]-amide, Compound 3: ZINC41016205: 2-(1,3-Dioxo-1,3-dihydro-isoindol-2-yl)-4-methyl-pentanoic acid [4-(4-fluoro-phenyl)-5-methyl-thiazol-2-yl]-amide, Compound 4: ZINC47160805: 2-(1,3-Dioxo-1,3-dihydro-isoindol-2-yl)-4-methyl-pentanoic acid [4-(4-fluoro-phenyl)-5-methyl-thiazol-2-yl]-amide. The structure of the hit compounds was depicted in Figure 1. The interacting residues for these molecules are shown in Table 1 and their structures are shown in Figure 2.

Figure 1: Chemical structures of the four lead molecules studied.

Figure 2: 3-D interaction representation of the top four hit compounds in the active site of the NMT. a) ZINC37555319, b) ZINC41016284, c) ZINC41016205, d) ZINC47160805.

Table 1: Glide extra-precision (XP) results for the four lead molecules, by use of Schrodinger 10.2.

The docking simulation of the four compounds within the binding site of the NMT was analysed and summarized in the following.

Binding mode of ZINC37555319

Compound ZINC37555319 had the least glide score and it exhibited one hydrogen bond interaction with NMT. The hydrogen atom of the SER 319 interacted with oxygen atom of the hit compound with bond distance (2.30Å). Two π - π stacking interactions were found between phenyl ring of ZINC37555319 with the hydrophobic residue of PHE 105 and PHE 103, increasing the stability of the ZINC37555319-NMT complex. The residues LEU 330, TYR 95, LEU 388, TYR 315, VAL 96, PHE 226 are mainly involved in hydrophobic interactions. The glide score and glide energy were calculated to be -10.20 kcal/mol, -81.74kcal/mol respectively.

Binding mode of ZINC41016284

Three hydrogen bond interactions were formed between NMT and ZINC41016284. The hydrogen atom of the ZINC41016284 compound interacted with backbone oxygen atom of GLY 199, GLY 386 with bond distance (2.07Å, 2.28Å, respectively). Beside the key residues, LEU 410, TYR 211, LEU 388, TYR 334, VAL 96, PHE 226, VAL 363 are mainly involved in hydrophobic interactions. The glide score and glide energy were calculated to be -10.15 kcal/mol, -88.81 kcal/mol respectively.

Binding mode of ZINC41016205

One hydrogen bond interaction was formed between ZINC41016205 and NMT. The backbone hydrogen atom of the GLY 199 interacted with an oxygen atom of ZINC41016205 with a bond distance of 2.02Å, Residues TYR 95, LEU 410, TYR 211, LEU 388, PHE 162, TYR 334, VAL 96, PHE 226, and VAL 363 are mainly involved in hydrophobic interactions. The glide score and glide energy were calculated to be -9.80 kcal/mol, -77.10 kcal/mol respectively, making ZINC41016205 the molecule with the fourth least binding energy free energy with NMT.

Binding mode of ZINC47160805

Three hydrogen bond interactions were formed between ZINC47160805 and NMT. The first one occurred in the side chain hydrogen atom of the polar residue ASN365, which tightly interacted with oxygen atom of the ZINC47160805 with a bond distance of 2.05 Å. The second is the backbone hydrogen atom of the GLY 199 interacted with oxygen atom of ZINC47160805 with a bond distance of 2.02Å. The third was between the hydrogen atom of the TYR with the oxygen atom of the ZINC47160805 with a bond distance of 2.45Å. Two π - π stacking interaction were found between the phenyl ring of ZINC47160805 with the hydrophobic residues, PHE 103 and HIS 213, increasing the stability of the ZINC47160805-NMT complex. Furthermore, the residues LEU 410, TYR 211, LEU 388, TYR 334, VAL 96,

PHE 226, VAL 363 were mainly involved in hydrophobic interactions. The glide score and glide energy were calculated to be -9.78 kcal/mol, -69.68 kcal/mol respectively.

ADME Properties prediction

Drug-like properties of the newly identified four hit molecules were assessed by QikProp to eliminate undesired drug-like compounds in the premature step of drug development process. The four hit molecules are fulfilled with drug-like properties based on Lipinski's rule of five, i.e. the molecular weights are < 500 kDa, there are < 5 hydrogen bond donors, <10 hydrogen bond acceptors, and the predicted octanol/water partition coefficient (QPlogPo/w) are <5. All these properties are well within the appropriate range of the Lipinski rule for drug-like molecules.

These hit compounds were further employed for further drug-like behaviour assessment by use of Qikprop. For the four hit molecules, cell permeability (QPPcaco2), a key factor governing drug metabolism and its access to biological membranes, ranged from ~126 to ~1864 nm/s (acceptable range: 25 is poor and 500 is great). The predicted IC₅₀ value for the blockage of HERG K⁺ channels is in the acceptable range below -5. The predicted Brain/Blood barriers are under acceptable range ~ -2.023 to -0.573, percentage of human oral absorption 84% to 100% (lower than 25 % is poor). All the pharmacokinetics parameters of the hit molecules fit well with the acceptable range and can be strongly recommended for drug research in humans. The results of ADME properties were reported in Table 2.

Table 2: Assessment of drug-like properties of the four hit molecules as verified by QikProp (Schrodinger 10.2).

Molecular Dynamic Simulation

In order to identify the stability, conformational changes and intermolecular interactions of the hit compounds with NMT, we executed the molecular dynamics simulation by assistance of

Desmond. It is noted that the RMSD plot of ZINC47160805 couldn't be obtained, suggesting the ZINC47160805-NMT is not stable, so only the stability studies of only three complexes were discussed in the following.

MD Trajectory analysis of ZINC37555319-NMT

The RMSD plot of the ZINC37555319-NMT complexes was depicted in Figure 3a, which indicate the slight conformational fluctuations in the complexes at the 27.90 ns and 98.50 ns. Reasonable RMSD values were noted as 1.61 Å, 1.80 Å respectively. Likewise, the slight deviation was observed in the ligand RMSD at the 28.80 ns and 92.80 ns, and the ligand RMSD were observed 1.49 Å, 1.50 Å respectively, even though these deviations didn't majorly effect deterioration of the ZINC37555319-NMT complex. The bar diagram (Figure 3b) of compound ZINC37555319 displayed hydrogen bond, hydrophobic, water bridge interactions. The residue ASN 364 (0.624) was mainly involved in the hydrogen bond interactions. Likewise, the water bridge and hydrophobic interactions were observed in the following residues PHE (0.851), (0.408) respectively. In addition, we observed the hydrogen bond interaction with ASN 365 with a maximum occupancy of 53%; three water bridge interactions were observed in the residues ASP 98, SERE 319, TYR 334, only one pi-cation interaction was observed between HIS 213 with furan ring of ZINC37555319, which elevated the binding stability of the protein-ligand complex during the simulation time (Figure 3c).

Figure 3: a) The RMSD plot of ZINC37555319-NMT complex during 100ns simulations. b) The bar diagrams of ZINC37555319-NMT contacts during 100ns simulations. c) The 2d diagram of ZINC37555319-NMT complex at end of the 100 ns simulations.

MD Trajectory analysis of ZINC41016284-NMT

The RMSD plot of the ZINC41016284-NMT complexes were depicted in Figure 4a, there was no fluctuation in the Protein RMSD up to 85 ns but slight conformational fluctuations were observed in the complexes at the 85.80 ns and the RMSD values were noted 2.15Å. Likewise, we examine the ligand stability, the deviation was slightly increased from 1.60 ns, 17.50 ns, 53 ns and 99.70 ns and the RMSD values were noted to be 3.69 Å, 3.96 Å, 4.53 Å, and 5.58 Å. The bar diagram (Figure 4b) of compound ZINC41016284 displayed hydrogen bond and water bridge interactions. The residues PHE 103 (0.748) and PHE 105 (0.613) were mainly involved in hydrophobic interactions, the water bridge interactions were observed in the residue ASP 98 (0.499). In addition, we observed the residues ASN 365 and PHE 103 being involved in hydrogen bond and pi-cation interactions, and residues ASP 98, HIS 213, SER 319, and TYR 334 were involved in water bridge interactions with maximum occupancies of 39%, 56%, 39%, 42%, 36%, and 49%, respectively, playing a significant role in the enhancement of the binding stability of the protein-ligand complex during the simulation time, as depicted in Figure 4c.

Figure 4: a) The RMSD plot of ZINC41016284-NMT complex during 100ns simulations. b) The bar diagrams of ZINC41016284-NMT contacts during 100ns simulations. c) The 2d diagram of ZINC41016284-NMT complex at end of the 100 ns simulations.

MD Trajectory analysis of ZINC41016205-NMT

The RMSD plot of the ZINC41016205-NMT complexes were depicted in Figure 5a, and slight conformational fluctuations were observed in the complexes at the 97.10 ns and the RMSD values were noted to be 1.92Å. Likewise, the deviation of ligand stability was slightly increased from 41.30 ns to 99.10 ns, and the RMSD values were noted 5.57 Å and 6.04 Å. The bar diagram (Figure 5b) of compound ZINC41016205 displayed hydrogen bond and water bridge interactions. The residue ASP 99 was mainly involved in hydrogen bond interactions with maximum occupancy 0.591. Likewise, water bridge interactions were observed in the

residues PHE 103 (0.814), ASP 385 (0.427). In addition, we observed residues ASP 99 and ASP 385 were involved in water bridge interactions with maximum occupancies of 33% and 51% , playing a significant role in the enhancement of the binding stability of the protein-ligand complex during the simulation time as reported in Figure 5c.

Figure 5: a) The RMSD plot of ZINC41016205-NMT complex during 100ns simulations. b) The bar diagrams of ZINC41016205-NMT contacts during 100ns simulations. c) The 2d diagram of ZINC41016205-NMT complex at end of the 100 ns simulations.

Conclusion

Malaria continues to be one of the major public health problems. In recent years, the mortality rate of malaria increased around the globe due to lack of effective treatment options to combat the increase in anti-malarial drug resistance. Several plasmodium species responsible for malaria, including the most common species in Sub-Saharan Africa, Plasmodium vivax, remain significant therapeutic targets for malaria. We have identified four potential inhibitors across the ZINC database through virtual screening, which include ZINC37555319, ZINC41016284, ZINC41016205, and ZINC47160805. These four compounds were studied for ADME properties prediction. Having the appropriate ADME properties, we further examined the dynamic behaviour of the three top-performing compounds, ZINC37555319, ZINC41016284, and ZINC41016205, using Desmond, which showed that the three compounds were stable in the dynamics simulation period. Through these computational investigations, we suggest that these three potential compounds are appropriate for further development of drug-like compounds.

Acknowledgements

The corresponding author would like to thank to Department of Biotechnology, Selvamm Arts and Science College, Namakkal for providing lab facilities as well as encouragement for this study.

Author Contributions

Conceived and designed the experiments: AM. performed the experiments: AM, MM. Analyzed the data: AM, AJ. Contributed software facility: AM. Wrote the paper: AM, H.-F.J., KJ. Assisted in writing the paper and referencing: H.-F. J, KJ.

Compliance with ethical standards

Not applicable. The ethical standards have been met

Funding

This compilation is a research article written by its author and required no substantial funding to stated.

Conflict of interest

The authors declare that they have no competing interests

Data availability

From corresponding authors upon request

Reference

1. <https://www.who.int/news-room/feature-stories/detail/world-malaria-report-2019>.
2. https://www.who.int/docs/default-source/malaria/world-malaria-reports/world-malaria-report-2020-briefing-kit-eng.pdf?sfvrsn=eda98467_9.
3. Jonathan Mawutor Gmanyami, Asiwome Ameko, Saviour Selase Ahiafe, Samuel Adolf Bosoka, Margaret Kweku, Evelyn Korkor Ansah.(2020). Effect of pre-consultation testing on clinicians' adherence to malaria test results and waiting time among children under 5 years in the Northern Zone of Volta Region of Ghana. *Malar J.* 19(1):120. doi: 10.1186/s12936-020-03189-6.

4. Marco A Biamonte , Jutta Wanner, Karine G Le Roch. (2013). Recent advances in malaria drug discovery. *Bioorg Med Chem Lett* ;23(10):2829-43. doi: 10.1016/j.bmcl.2013.03.067.
5. Nureni Olawale Adeboye, Olawale Victor Abimbola, Sakinat Oluwabukola Folorunso . (2019). Malaria patients in Nigeria: Data exploration approach. *Data Brief* ;28:104997. doi: 10.1016/j.dib.2019.104997.
6. Tayo O Olaleye , James A Brannigan, Shirley M Roberts, Robin J Leatherbarrow, Anthony J Wilkinson, Edward W Tate. (2014). Peptidomimetic inhibitors of N-myristoyltransferase from human malaria and leishmaniasis parasites. *Org Biomol Chem*;12(41):8132-7. doi: 10.1039/c4ob01669f.
7. Anja C Schlott , Anthony A Holder , Edward W Tate . (2018). N-Myristoylation as a Drug Target in Malaria: Exploring the Role of N-Myristoyltransferase Substrates in the Inhibitor Mode of Action. *ACS Infect Dis*. 4(4):449-457. doi: 10.1021/acsinfecdis.7b00203.
8. Megan H Wright, Barbara Clough, Mark D Rackham, Kaveri Rangachari, James A Brannigan, Munira Grainger, David K Moss, Andrew R Bottrill , William P Heal, Malgorzata Broncel, Remigiusz A Serwa, Declan Brady, David J Mann, Robin J Leatherbarrow , Rita Tewari, Anthony J Wilkinson, Anthony A Holder, Edward W Tate . (2014). Validation of N-myristoyltransferase as an antimalarial drug target using an integrated chemical biology approach. *Nat Chem*. 6(2):112-21. doi: 10.1038/nchem.1830.
9. Marco A Biamonte , Jutta Wanner, Karine G Le Roch. (2013). Recent advances in malaria drug discovery. *Bioorg Med Chem Lett* ;23(10):2829-43. doi: 10.1016/j.bmcl.2013.03.067.
10. Mohammad Hassan Baig, Khurshid Ahmad, Gulam Rabbani, Mohd Danishuddin, and Inho Choi. (2018). Computer Aided Drug Design and its Application to the Development of

Potential Drugs for Neurodegenerative Disorders. *Curr Neuropharmacol.* 16(6): 740–748. doi: 10.2174/1570159X15666171016163510.

11. Victor Goncalves, James A Brannigan, David Whalley, Keith H Ansell, Barbara Saxty, Anthony A Holder, Anthony J Wilkinson, Edward W Tate, Robin J Leatherbarrow. (2012). Discovery of Plasmodium vivax N-myristoyltransferase inhibitors: screening, synthesis, and structural characterization of their binding mode. *J Med Chem*;55(7):3578-82. doi: 10.1021/jm300040p.
12. Mohan Anbuselvam, Murugesh Easwaran, Arun Meyyazhagan, Jeeva Anbuselvam, Haripriya Kuchi Bhotla, Mathumathy Sivasubramanian, Yamuna Annadurai, Tanushri Kaul, Manikantan Pappusamy, Balamuralikrishnan Balasubramanian. (2020). Structure-based virtual screening, pharmacokinetic prediction, molecular dynamics studies for the identification of novel EGFR inhibitors in breast cancer. *J Biomol Struct Dyn*;1-10. doi: 10.1080/07391102.2020.1777899.
13. Irwin, J. J., & Shoichet, B. K. (2005). ZINC – a free database of commercially available compounds for virtual screening. *Journal of Chemical Information and Modeling*, 45(1), 177–182. <https://doi.org/10.1021/ci049714> <https://doi.org/10.1021/ci049714>.
14. Kh. Dhanachandra Singh, Muthusamy Karthikeyan, Palani Kirubakaran, SelvaramanNagamani (2011) Pharmacophorefiltering and 3D-QSAR in the discovery of new JAK2 inhibitors. *Journal of Molecular Graphics and Modelling*. 30: 186–197.13.
15. Saravana Prabha Poochi, Murugesh Easwaran, Balamuralikrishnan Balasubramanian, Mohan Anbuselvam, Arun Meyyazhagan, Sungkwon Park, Haripriya Kuchi Bhotla, Jeeva Anbuselvam, Vijaya Anand Arumugam, Sasikala Keshavarao, Gopalakrishnan Velliyur Kanniyappan, Manikantan Pappusamy, Tanushri Kaul. (2020).Employing bioactive compounds derived from *Ipomoea obscura* (L.) to

- evaluate potential inhibitor for SARS-CoV-2 main protease and ACE2 protein. Food Front. 10.1002/fft2.29. doi: 10.1002/fft2.29.
16. Schrodinger Release–2: Qikprop, Schrodinger, LLC, New York, NY, 2020.
 17. Anbuselvam Mohan, Anbuselvam Jeeva, Azhagiya Manavalan Lakshmi Prabha, Sukumar Sumathi, Elumalai Murugan. (2012). In silico docking studies of Berchemia lineate compounds against human prostate cancer protein PTEN. Journal of Pharmacy Research 2012, 5(8),4492-4495.
 18. Lakshmanan, L, Karthikeyan, M. Investigation of Drug Interaction Potentials and Binding Modes on Direct Renin Inhibitors: A Computational Modeling Studies. Lett. Drug. Des. Discov., 2019, 16, 8, 919-938.
 19. Gharaghani S, Khayamian T, Keshavarz F. (2012) Docking, Molecular Dynamics Simulation Studies, and Structure based QSAR Model on Cytochrome P450 2A6 Inhibitors. Struct. Chem. 23, 341–350.
 20. RaminEkhteiriSalmas, AyhanUnlu, MuhammetBektaş, Mine Yurtsever, MertMestanoglu& Serdar Durdagi. (2017). Virtual Screening of Small Molecules Databases for Discovery of Novel PARP-1 Inhibitors: Combination of in silico and in vitro Studies. J Biomol Struct Dyn.35(9):1899-1915. doi: 10.1080/07391102.2016.1199328.

Table 1: Glide extra-precision (XP) results for the four lead molecules, by use of Schrodinger 10.2.

S. No	Compound ID	Glide score	Glide Energy	No. of hydrogen	Interaction residues	Distance (Å)

				bonds		
1	ZINC37555319	-10.20	-81.74	1	SER 319	2.30
2	ZINC41016284	-10.15	-88.81	2	GLY 386, GLY 199	2.28, 2.07
3	ZINC41016205	-9.80	-77.10	1	GLY 199	2.02
4	ZINC47160805	-9.78	-69.68	3	ASN 365, TYR 334	2.05, 2.45

The Compound IDs are labelled as such under the ZINC database; Glide score (Kcal/mol), Glide energy (Kcal/mol), No of hydrogen bond interaction, Interacting residues, Distance between the protein and ligand (Å).

Table 2: Assessment of drug-like properties of the four hit molecules as verified by QikProp (Schrodinger 10.2).

Compound ID	MW	HBD	HBA	QPLogPo/w	Caco-2	QPLogHERG	QPLogB/B	% Oral absorption
ZINC37555319	438.525	1.000	6.000	5.267	1864	-6.016	-0.600	100
ZINC41016284	479.611	1.000	8.500	4.248	126	-6.415	-2.023	89
ZINC41016205	451.514	1.000	7.000	4.998	1203	-6.676	-0.573	100
ZINC47160805	402.452	1.000	8.500	2.335	271	-4.438	-1.333	84

Molecular weight (<500 Da). Hydrogen bond donors (<5). Hydrogen bond acceptors (<10).

Predicted octanol/water partition co-efficient log p (acceptable range: 22.0 to 6.5). Predicted

Caco-2 cell permeability in nm/s (acceptable range: 25 is poor and .500 is great). Predicted

IC50 value for blockage of HERG K⁺ channels (concern: below -5). QP log BB for

brain/blood (-3.0 to 1.2). Predicted percentage of human oral absorption (25 % is poor).

Figure 1: Chemical structures of the four lead molecules studied.

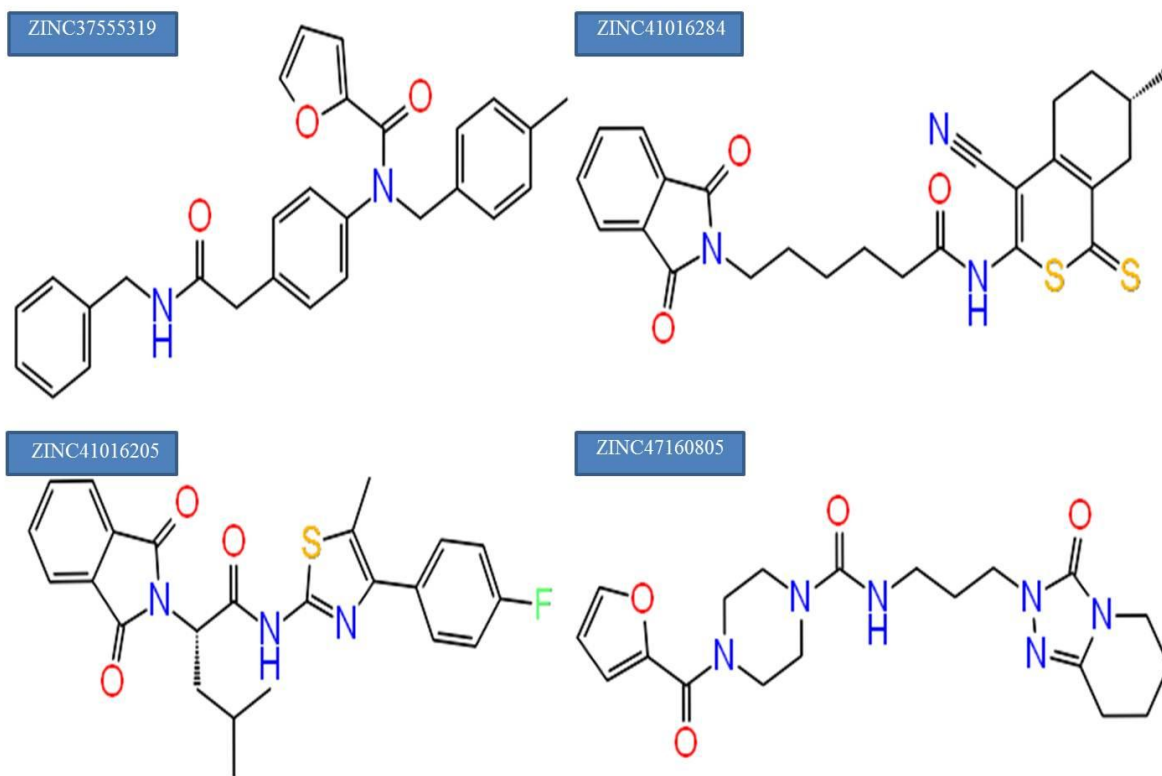
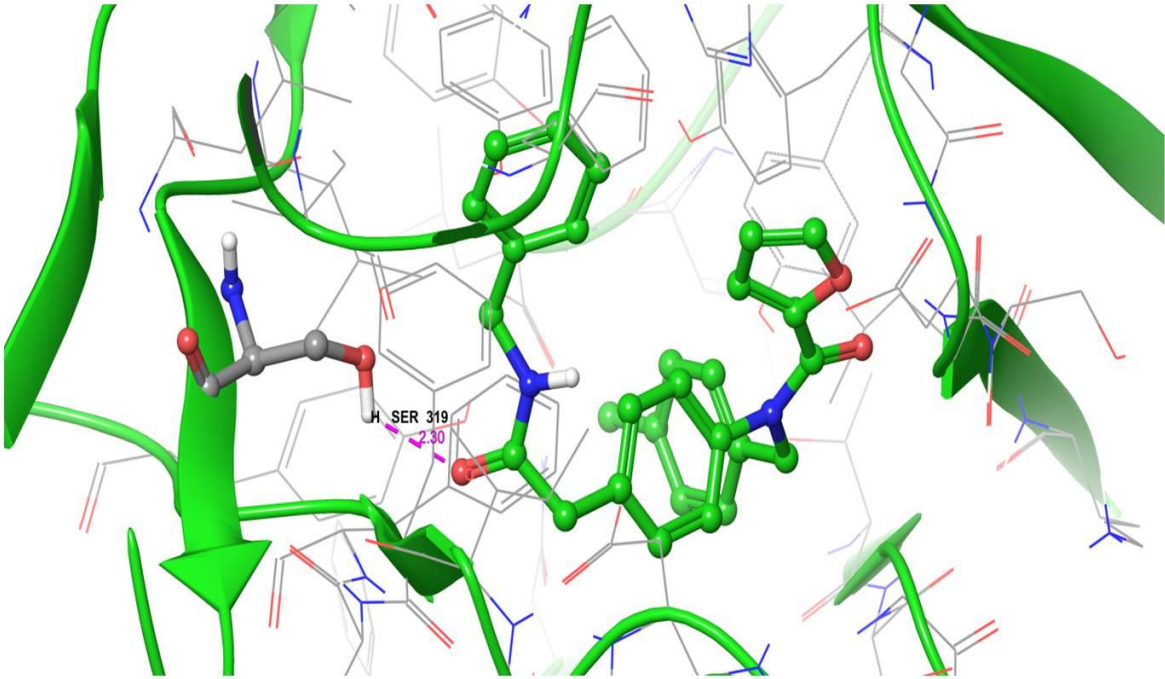
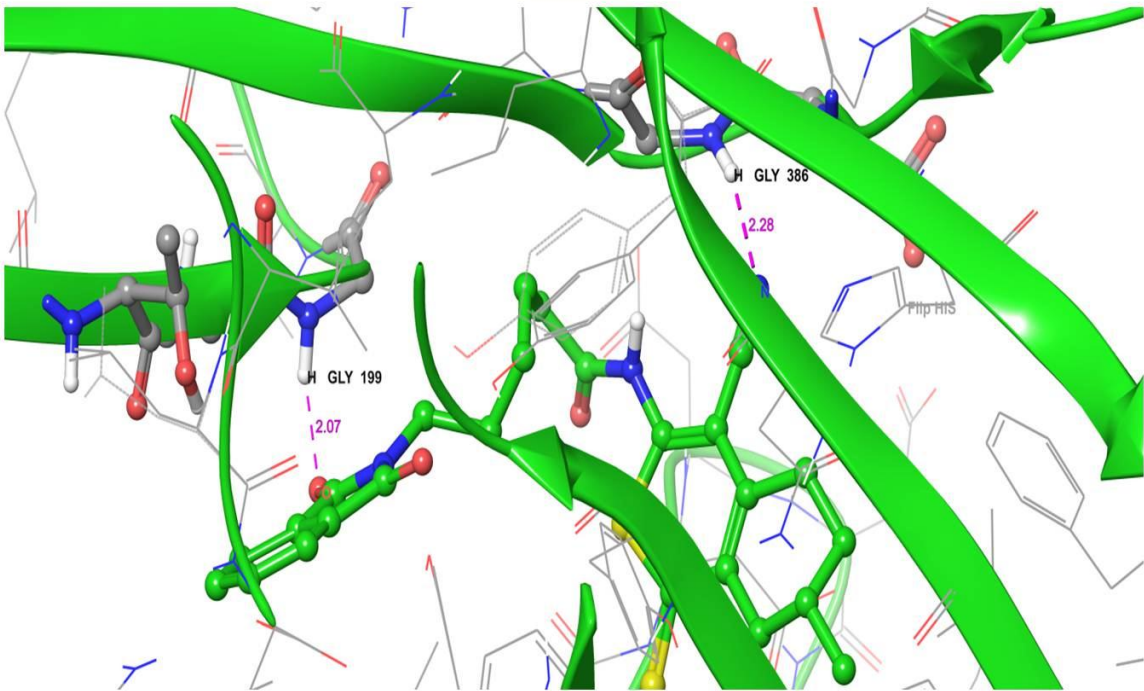


Figure 2: 3-D interaction representation of the top four hit compounds in the active site of the NMT. a) ZINC37555319, b) ZINC41016284, c) ZINC41016205, d) ZINC47160805.

2a



2b



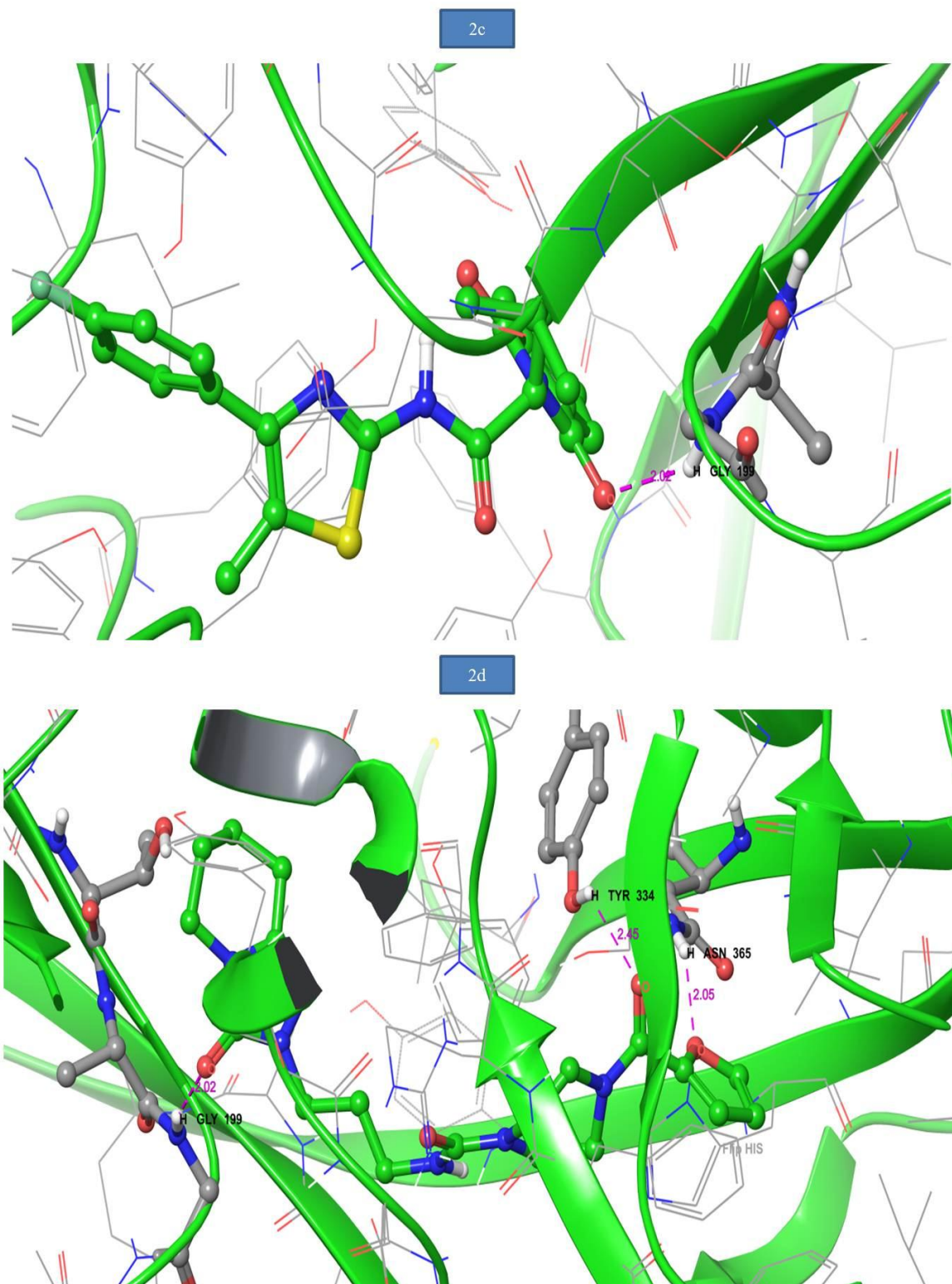
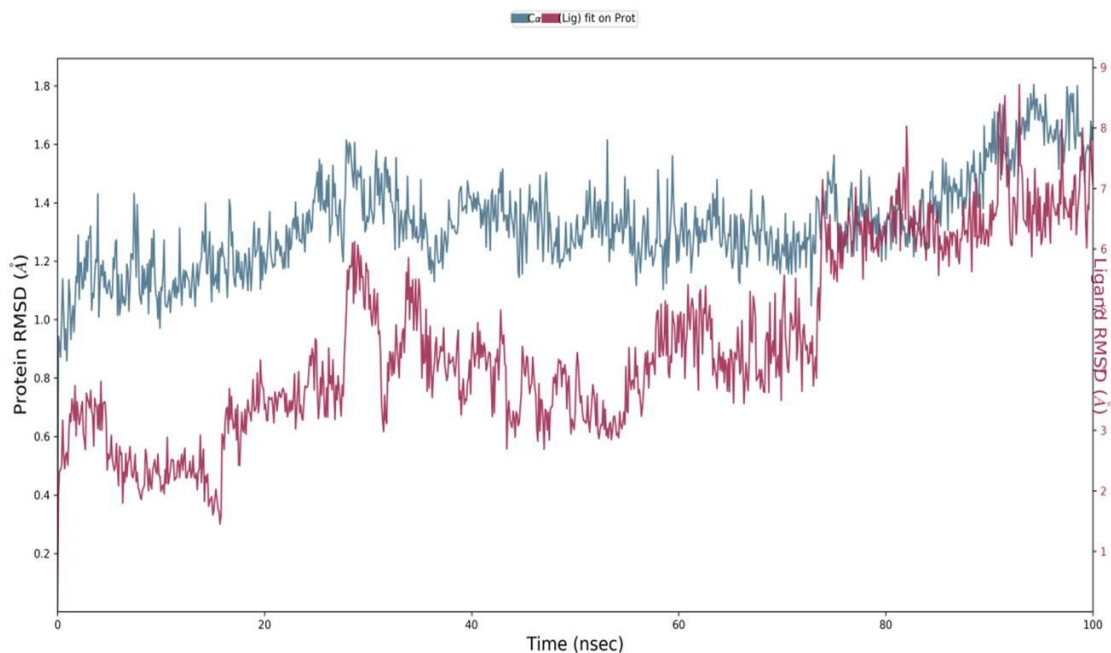
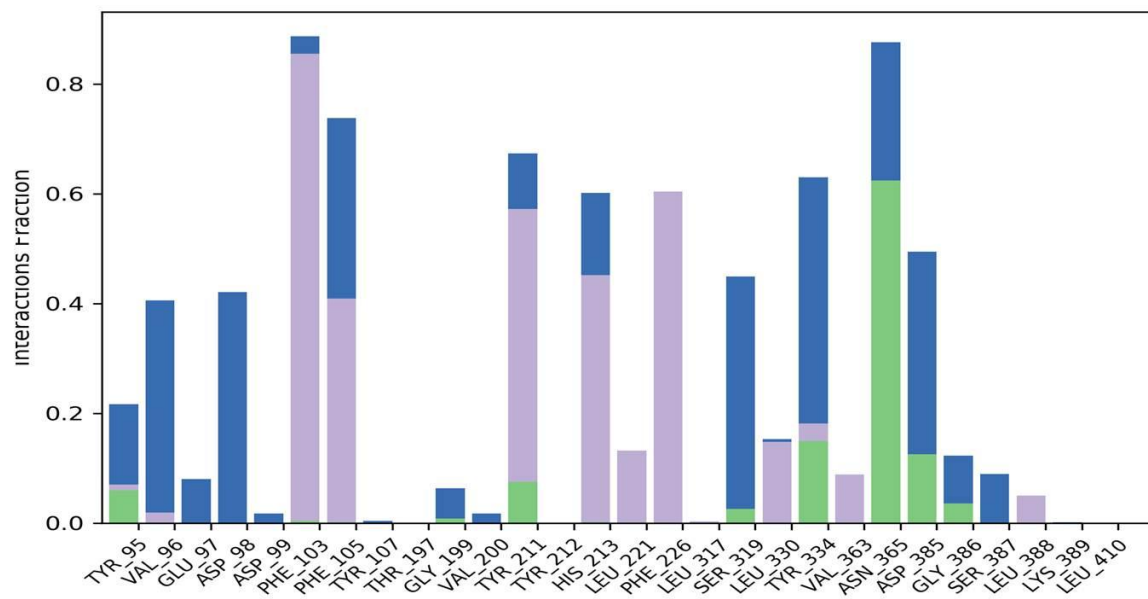


Figure 3: a) The RMSD plot of ZINC37555319-NMT complex during 100ns simulations. b) The bar diagrams of ZINC37555319-NMT contacts during 100ns simulations. c) The 2d diagram of ZINC37555319-NMT complex at end of the 100 ns simulations.

3a



3b



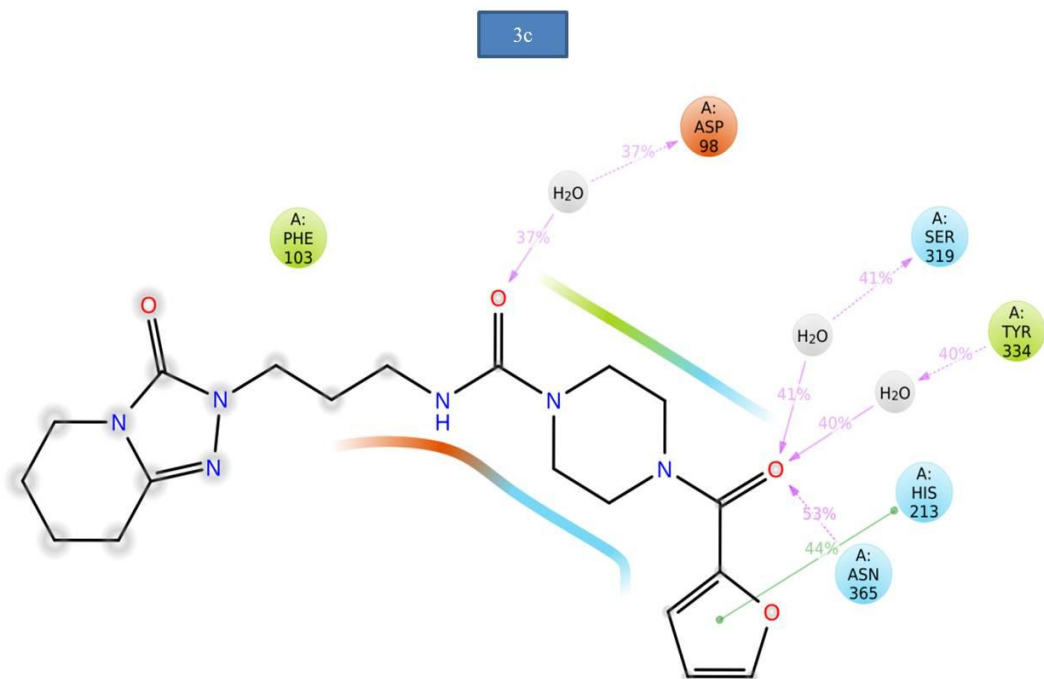
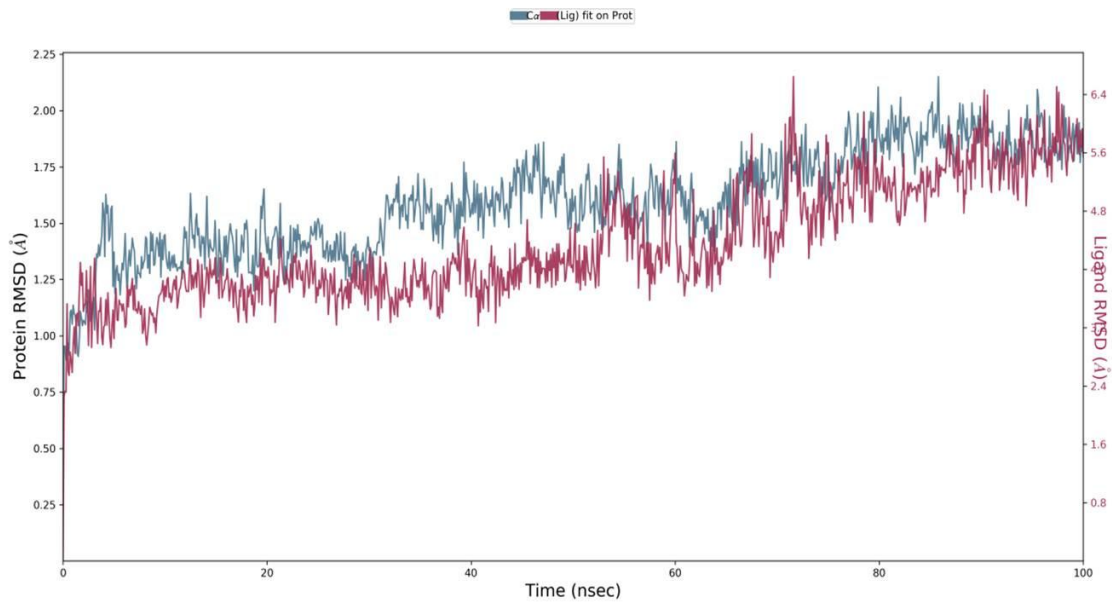
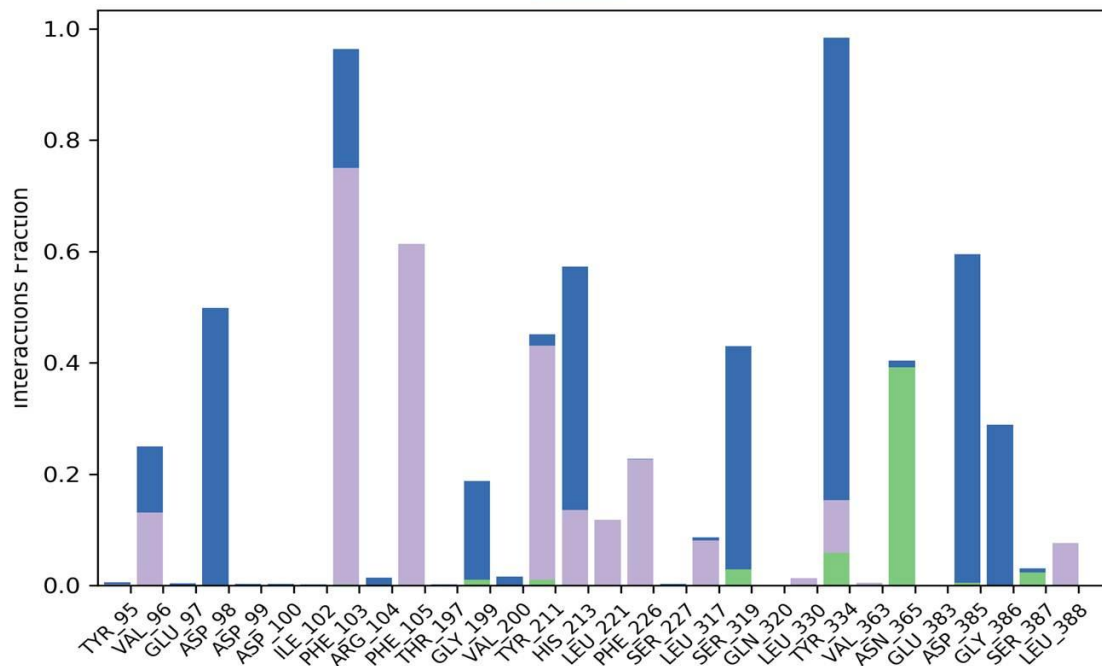


Figure 4: a) The RMSD plot of ZINC41016284-NMT complex during 100ns simulations. b) The bar diagrams of ZINC41016284-NMT contacts during 100ns simulations. c) The 2d diagram of ZINC41016284-NMT complex at end of the 100 ns simulations.

4a



4b



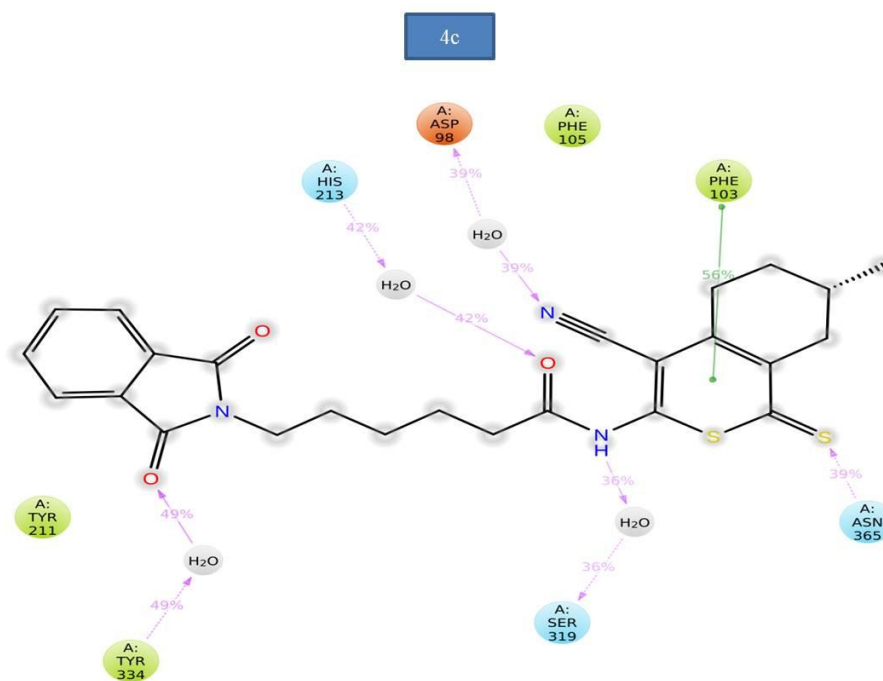
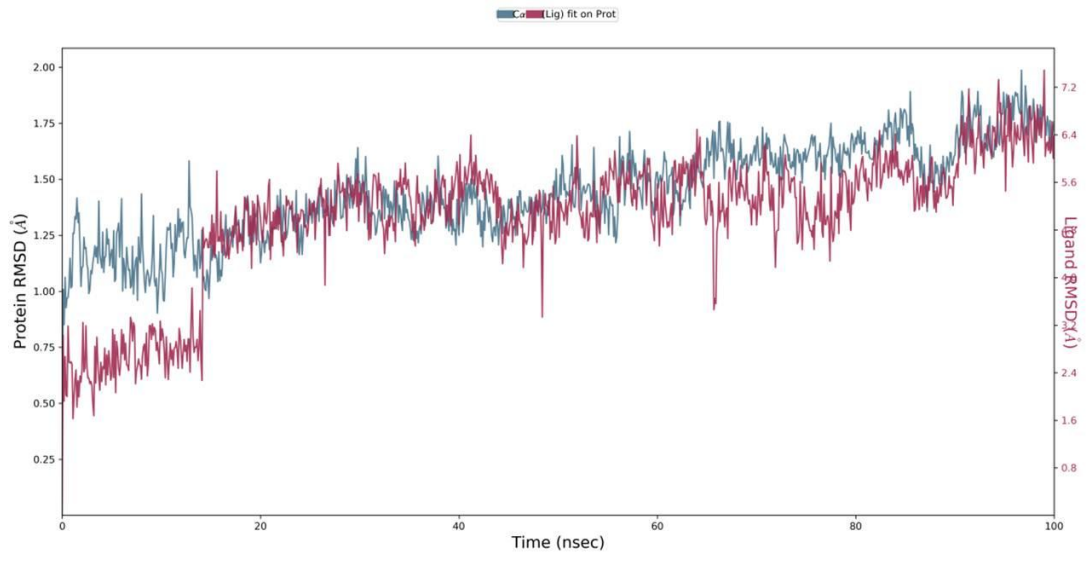
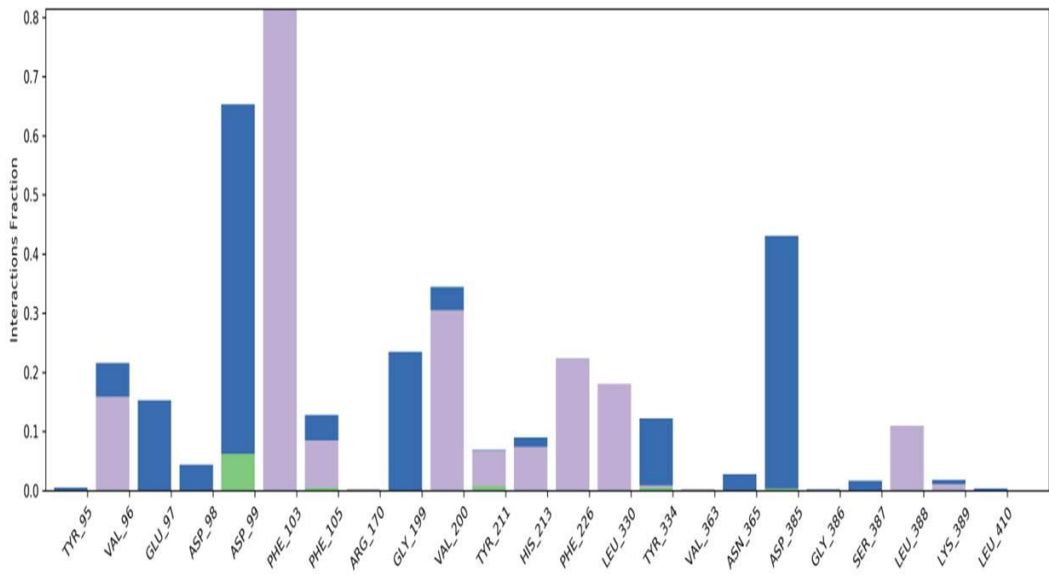


Figure 5: a) The RMSD plot of ZINC41016205-NMT complex during 100ns simulations. b) The bar diagrams of ZINC41016205-NMT contacts during 100ns simulations. c) The 2d diagram of ZINC41016205-NMT complex at end of the 100 ns simulations.

5a



5b



5c

